

High piezoelectric actuation response in graded Nd_2O_3 and ZrO_2 doped BaTiO_3 structures

Relva C. Buchanan · Eusiu Park · Rajesh Surana ·
Harshani Tennakone · Kirthi Tennakone

Received: 9 December 2009 / Accepted: 22 March 2011 / Published online: 9 April 2011
© Springer Science+Business Media, LLC 2011

Abstract High electromechanical strains have been developed in this study in Barium Titanate ceramics, suitably doped with Nd and Zr to form a controlled concentration gradient, leading to a dome-like structure on sintering. Compacted pellets constituted of layers of barium titanate powder of varying minor amounts of Nd and Zr powders, incorporated as nitrates precursors, acquire this dome shape on sintering at 1300–1320°C and cooling to the ambient temperature, the result of the residual thermoelastic strain. The dome structures exhibit high electromechanical responses, and the piezoelectric coefficients (deduced from electric field induced strains measurements in dome-up and dome-down positions) are also found to be exceptionally high. These Nd and Zr doped barium titanate structures could find applications as an environmentally benign material for fabrication of high displacement functionally graded electromechanical actuators in a single sintering step process.

Keywords Piezoelectric actuator · High strain · Barium titanate · Neodymium oxide · Zirconium oxide

1 Introduction

Piezoelectric and electrostrictive polycrystalline ceramics, are widely used in sensor and actuator devices [1, 2]. The conventional materials of this category possess high frequency response and low hysteresis, but the strains are

low and limited to about 0.1% at 10 kVcm^{-1} . Different techniques have been developed for fabricating large displacement actuators using monomorph or bimorph benders, RAINBOW, single crystals, relaxor based systems such as PMN-PT, formulated near the morphotropic phase boundaries [3–13]. In unimorphs and bimorphs, the bonding interface has low strength. Also large discontinuities in stress and chemical concentration appear near the bonding interface, due to the difference of material properties of the passive and piezoelectric components, resulting in alteration of their characteristics. The stress, the large concentration gradients and structural weakness at the bonding interface deteriorate bimorph and unimorph actuators in cyclic actuation. To increase the reliability of bending actuators, RAINBOW structures were proposed. The RAINBOW type high displacement actuators are made by creating a reducing gradient in the PZT material. In the RAINBOWs, the chemically integrated reduced and piezoelectric layers exhibit high strength, therefore the device performs more durably. However, the toxicity of lead demands use of more environmentally friendly materials, for use in these electromechanical systems.

Barium Titanate (BT) is a widely used low cost and environmentally benign electroceramic material of versatile adaptability. Recently, functionally graded actuator systems have attracted much attention [14–16]. In this paper, fabrication of graded electromechanical actuators from Nd and Zr doped BT was explored. The material, in the form of discs displaying electromechanical amplification, were made by compacting the BT precursor powders, doped with additive Nd_2O_3 and ZrO_2 at different concentrations, to form two or three distinct layer structures, followed by sintering to form discrete graded structures. During the sintering process, the differential thermal expansion of the layers warps the disc to a dome shape, and this curvature is

R. C. Buchanan (✉) · E. Park · R. Surana · H. Tennakone ·
K. Tennakone

Department of Chemical and Materials Engineering,
University of Cincinnati,
Cincinnati, OH 45221-0012, USA
e-mail: buchanrc@ucmail.uc.edu

retained on cooling, due to residual stress. This anisotropic stress state leads to preferred domain orientation (hence the high spontaneous polarization), which when switched by the electric field results a significant strain difference that alters the curvature of the dome. The effective piezoelectric coefficients d_{33} and d_{31} can then be estimated from the observed electric field induced curvature changes of the dome.

2 Experimental

The starting material used in all experiments was high purity BaTiO₃ (Ticon-HPB, Ferro Corp) with a stoichiometric excess of Ti (Ba/Ti ratio=0.997), impurity concentration of SrO₂, SiO₂, Al₂O₃ and Fe₂O₃ less than 0.1% and the average particle size 1.23 μm . The dopants, Nd₂O₃ and ZrO₂ were introduced in the form of nitrates Nd(NO₃)₃.xH₂O and ZrO(NO₃)₂.xH₂O (Aldrich), dispersed in a solvent mixture of 40 vol. % de-ionized water and 60 vol. % isopropanol, after estimating the respective oxide content. The slurry with added binders was ball milled for 12 h, spray dried to a dry powder containing BT and the dopants. A weighed amount (0.25 g) of the powder was pressed at 7×10^6 Pa and the next layer pressed on top of the first initially at the same pressure and after 20 s pause, pressure increased to 21×10^6 Pa. Three layer green pellets were prepared in the same manner. Samples were fired at 1300–1315°C for 90 min, and allowed to cool. Samples processed as above were dome shaped. After recording the dimensions (a_o =rim diameter; h_o =height of the inner convex cap, t_o =thickness) both surfaces were electroded by Al evaporation. Capacitance at 1 kHz was recorded using Hewlett-Packard LCZ meters (Models 4276A and 4194 A). Electric field induced strain response was measured by placing the specimen in a plastic container filled with silicone oil and strain was recorded as the induced field was varied. A linear variable differential transformer (LVDT) Lucas Schaevitz Model MP-2000 was used as the displacement sensor. The sensor was calibrated using a Schaevitz LBB-100 gauge head with sensitivity 200 V/V/cm, following the procedure prescribed by the manufacturer. During calibration the voltage was varied from -0.15 to +0.15 using a Trek power supply and the plot of LVDT position vs. voltage was plotted and found to be accurately linear ($r^2=0.99998$). In measuring the field induced displacement of the samples, sinusoidal 10 s voltage pulses were induced using a Wavetek Model 29 Function Generator. For confirmation of the calibration 0.76 mm thick EDO EC-76 PZT plate was also tested, yielding specified butterfly strain responses (0.1 to -0.3%) and $d_{33} \sim 236 \text{ pCN}^{-1}$. For all dome samples, measurements were made using the dome-down as well as the dome-up positions, keeping the LVDT probe at the apex (Fig. 1).

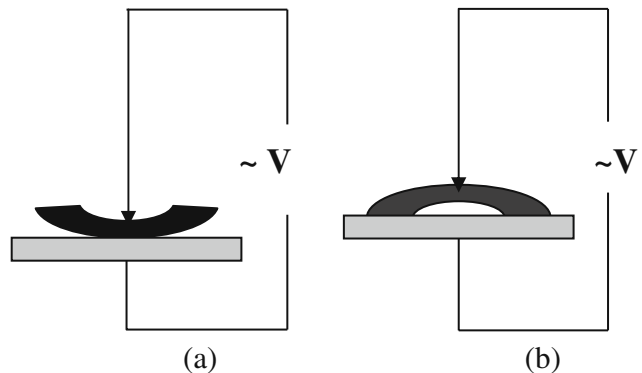


Fig. 1 Strain measurement (a) dome-downward (b) dome-upward position

3 Results and discussion

BT doped with trivalent rare earth oxides generally exhibits semiconductivity at low (< 0.05 m/o) doping concentrations and a PTCR effect is typically seen in polycrystalline samples [17–19]. On increasing the doping concentration, the material transforms to an insulating phase, owing to the change in the compensation mechanism from electronic to ionic charge balance. Similar behavior is observed in Nd₂O₃ doped BT. A notable feature of Nd compared to other rare earth dopants is that, its ionic radius lies almost mid way between that of Ba and Ti, allowing possible substitutions at both A and B sites in BaTiO₃ [20, 21]. The possibility of both A and B substitutions makes Nd doped BT an interesting material and promising dielectric properties have been noted [20–23]. Doping of the BT with ZrO₂ is known to modulate the microstructure, as well as the dielectric and electromechanical properties [24–27]. Generally, ZrO₂ segregates to the grain boundaries forming core-shell structures with BT cores and BaTi_{1-x}Zr_xO₃ shells, where Ti is partially replaced by Zr [24–26]. When BT is doped individually with Nd and Zr at varying concentrations, significant changes in field induced strain beyond that of BT was not observed at 10–15 kV/cm. There are, however, indications of higher strains at lower field strengths corresponding to the higher values of $d_{33} \sim 283 \text{ pCN}^{-1}$ in samples doped with 2.0 m/o ZrO₂, compared to $\sim 90 \text{ pCN}^{-1}$ for the un-doped BT samples, an effect observed by other workers [26]. In co-doped samples with 1–2 m/o Zr, the strain increased with increase of Nd and exceeded 0.2% per 10 kV at an optimal doping concentration (Nd₂O₃=0.6 m/o, ZrO₂=1 m/o). Again Nd and Zr doping alters the density of the BT owing to changes in lattice parameters. In Nd doping, density decreases sharply when the concentration exceeds ~ 0.5 –0.6 m/o. The opposite happens if the samples are also co-doped with Zr, i.e., density of Nd doped BT increases on increase of the Zr concentration. Clearly symmetric structures do not produce warping, however even in a homogeneous Nd/Zr doped pellets

some warping is noticed because of the uneven oxidation in two faces of a pellet. If the oxidized outer layer on one face of the pellet is removed and heated again, the pellet acquires a dome shape (Fig. 2). The effect is further magnified when a compositional variation is introduced to form layers.

The electromechanical displacement of a dome-shaped actuator depends on its geometry and the piezoelectric properties of the material [28]. On this basis, a series of experiments conducted with pellets composed of two and three layers of differently doped BT, high actuation properties were observed in the two-layer and three layer systems, as indicated in the Fig. 3 (a), (b).

Figure 3(c) shows a magnified optical image of a diametrical cross-section of the sintered two-layered pellet. The highly Nd doped region of the pellet bends to the concave side of the dome because of the relative volume contraction of ~1.3% after sintering and cooling. On application of an electric field, the piezoelectric strains developed change the curvature of the dome. If the sample is positioned dome-up and the probe placed on the apex of the convex surface (Fig. 1(b)), the observed strain response can be related to applied voltage as follows.

The deformative response $Z(r;\theta)$ of a disc of piezoelectric material due to an electric field applied normal to surface is described by the equation [29, 30],

$$\nabla^4 Z = -\nabla^2 V \quad (1)$$

where: $V(r;\theta)$ is the potential distribution over the surface . For a constant potential distribution, solution of (1) gives curvature of deformation κ as [30].

$$\kappa = [12d_{31}V(t_1 + t_2)]/At^3 \quad (2)$$

where,

$$A = 4 + 6(t_2/t_1) + 4(t_2/t_1)^2 + (E_2/E_1)(t_2/t_1)^3(1 - \nu_1)(1 - \nu_2)^{-1} \quad (3)$$

$$+ (E_1/E_2)(t_1/t_2)(1 - \nu_2)(1 - \nu_1)^{-1}$$

t_1, t_2 =thickness of the active, passive layers

E_1, E_2 =Young's moduli of the active, passive materials
 ν_1, ν_2 =Poisson's ratio of the active, passive materials

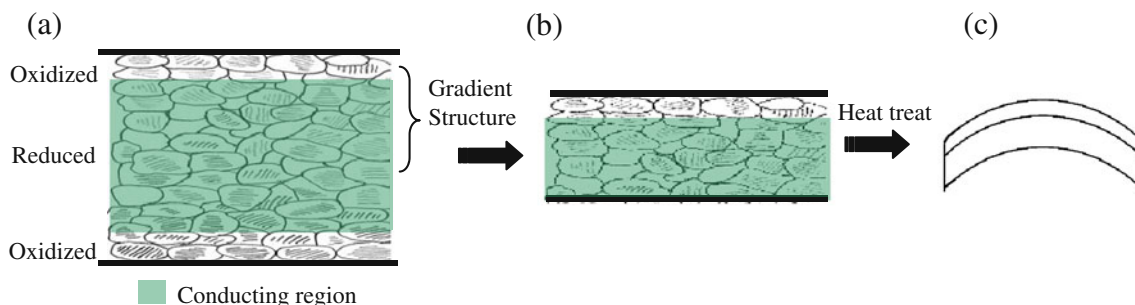


Fig. 2 Barrier Layer gradient structure (a) symmetric (b) asymmetric (c) dome formation after heat treatment

Warping of the disc during sintering and further curvature changes on application of the electric field indicates the existence of gradients in the thermoelastic and piezoelectric properties. The system as modeled in effect constituted two equally thick piezoelectrically active and passive layers. On setting $E_1=E_2, \nu_1=\nu_2, t_1=t_2=t/2$ (t = thickness of the disc), the expression (2) for the curvature of the disc simplifies to,

$$\kappa = 6d_{31}V/t^2 \quad (4)$$

After sintering and cooling the sample acquires a dome shape of height h_o , rim radius a_o and radius of curvature r_o , on application of the electric field these parameters changes to h_V, a_V and r_V respectively (Fig. 4)

The unclamped disc is not subjected to external stresses other than those originating from the applied electric field and the deformation caused by domain orientation conserves volume. Assumption that the volume of the disc is conserved in the electric field induced deformation, leads to the constraint,

$$r_o h_o t_o \simeq r_V h_V t_V \quad (5)$$

where t_o, t_V and r_o, r_V are the thicknesses and radii of curvature of the disc before and after application of the electric field.

Using (4), the curvatures of the disc before and after application of the electric field can be expressed as,

$$1/r_o = 6e/t_o^2, 1/r_V = 6(e - d_{31}V)/t_V^2 \quad (6)$$

Where, e =residual strain in the warped disc after sintering and cooling and $t_V=t_o+d_{33}V$

Eliminating the unknown quantity e , (5) can be written as,

$$h_V = h_o - [(6d_{31}r_o h_o)/t_o^2 + 3(d_{33}h_o)/t_o]V + [(18r_o h_o d_{31}d_{33})/t_o^3]V^2 \quad (7)$$

The lengths r_o and h_o are connected by the geometrical identity $h_o^2 + a_o^2 = 2r_o h_o$.

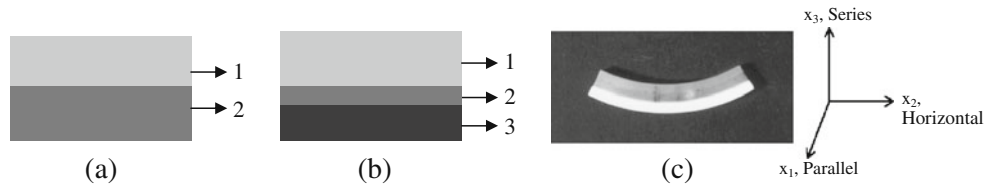


Fig. 3 (a) Two and (b) three layer pellets. ZrO₂ doping concentration is kept constant at 2 mol% and Nd₂O₃ content varied from 0.05 to 0.3 m/o. Wt. of powder is 0.25 g in the layers 1 and 2 of (a) and 0.2,

The observed strain response of the dome in the upward position then takes the form,

$$(h_V - h_o)(h_o + t_o)^{-1} = - \left[(6d_{31}r_o h_o)/(h_o + t_o)^{-1} t_o^{-2} + 3(d_{33}h_o)/(h_o + t_o)^{-1} t_o^{-1} \right] V + \left[(18r_o h_o d_{31} d_{33})(h_o + t_o)^{-1} t_o^{-3} \right] V^2 \quad (8)$$

Figure 5 shows the butterfly curves obtained and the strain response induced by the applied field, the strain measurements in dome-down and up positions and an axial strain of ~0.4–0.6% at 10 kV cm⁻¹ observed in the dome-down position. The dimensions of the dome shaped pellet as in Fig. 3(c) were as follows; rim radius $a_o=0.28$ cm, height of the inner spherical cap $h_o=0.04$ cm and, thickness $t_o=0.11$ cm. The gradient (G) of Eq. 8 at V=0 given by;

$$G = - \left[(6d_{31}r_o h_o)/(h_o + t_o)^{-1} t_o^{-2} + 3(d_{33}h_o)/(h_o + t_o)^{-1} t_o^{-1} \right] \quad (9)$$

This expression (Eq. 9) enables calculation of d_{31} , as d_{33} is already available from dome-down measurements. From the curve of dome-up position in Fig. 5(a), G=0.097 cm/kV, and h_o , a_o , r_o values provided a d_{31} value of 325

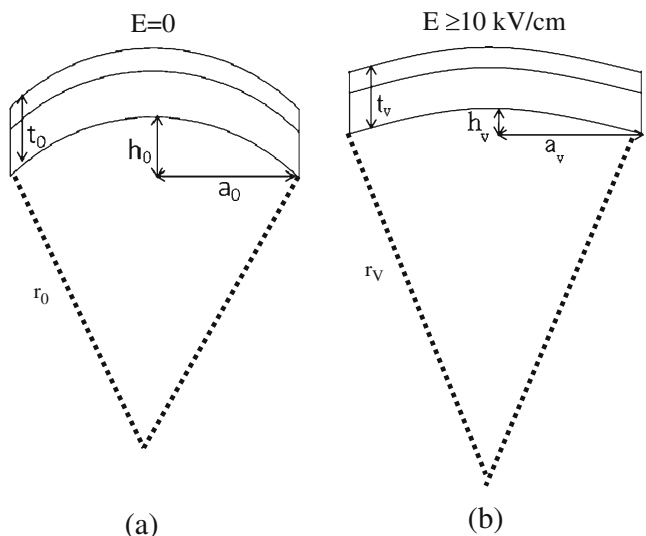


Fig. 4 Change in curvature of the dome shaped disc formed after heat treatment with (a) with no application of an electric field, E=0 and (b) with $E \geq 10$ kV/cm

0.1, 0.2 g respectively in the layers 1, 2, 3 in (b). (c) Magnified optical image of the cross-section of the pellet after heating and cooling

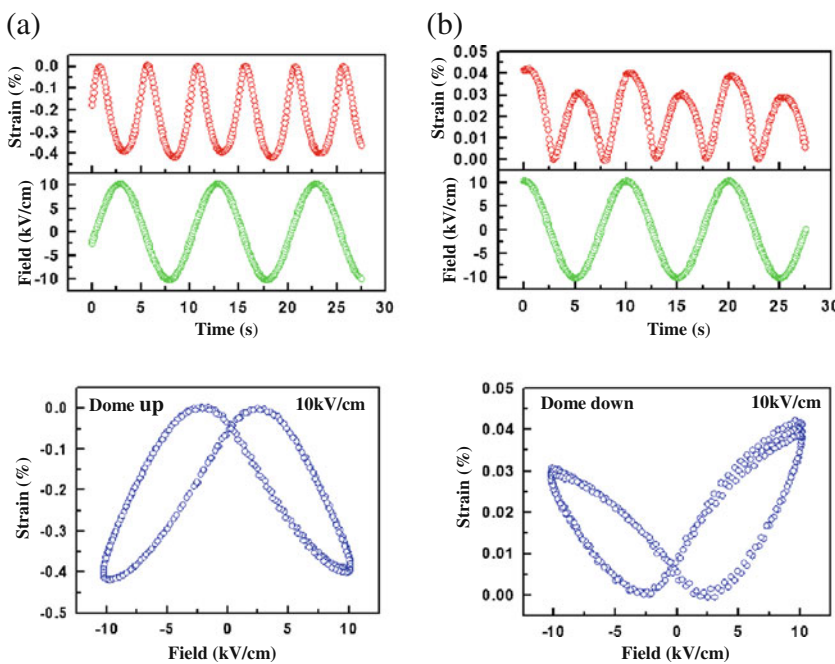
pCN⁻¹. From the gradient in Fig. 5(b) (0.00526), the effective piezoelectric constant can be estimated. The resultant calculated values: $d_{33}=526$ pCN⁻¹ and d_{31} (=325 pCN⁻¹) obtained are quite high and comparable to values for the best PZT systems. In the case of uniformly doped pellets d_{33} values obtained from the strain measurements were lower than that of the domed samples. In dome shaped samples, strain resulting from deformation increases the effective d_{33} . From (8) it is evident that displacement of the actuator depends on d_{31} and d_{33} , but the d_{33} effect is negligible when $r_o/t_o > d_{33}/6d_{11}$, a condition which is almost always satisfied. It is important to note that the coefficient of V in (8) depends on d_{33} because the rim of disc has freedom to move. In a disc clamped along the rim, this coefficient depends only on d_{31} and the d_{33} effect on displacement is second order. Again, the displacement increases when the initial radius of curvature (r_o) of the dome is increased and thickness (t_o) decreases. A high initial curvature indicates that the material is in a stressed condition, and such internal stress generally leads to higher values of piezoelectric coefficients. A more stretched compositional distribution across the thickness of the disc would develop higher strains. However, there is no clear quantitative basis for determining the conditions that favor optimum displacement.

The strain characteristics of three layered system (a thin layer of BT doped with 0.01 mol % Nd₂O₃ and 2.0 m/o ZrO₂ in the middle, Fig. 3(b)) in the dome-down position is shown in Fig. 6. Here the strain is 1.2% at 10 kV cm⁻¹ compared 0.6% for the previous case (Fig. 5(b)).

The above results clearly indicate that the sensitivity of the electromechanical amplification depends on the nature of the compositional gradient. In the three-layer system, the more complex graded structure that is developed gives a higher electromechanical response, compared to the two-layered system. Here, the compositional gradient approximates more to a continuous one, especially if the layers are sufficiently thin. However, optimization of the three-layer system was found to be difficult because of the combinatorics involved and constraint on the pellet thickness.

The dielectric constants of the samples were in the range 2000–3000 at 1 kHz with losses of the order 0.01–0.02. Although the D.C resistivity of the samples were quite high

Fig. 5 Strain responses of Nd/Zr doped, 0.11 cm thickness two layered structure, (a) dome up (b) dome down at 0.1 Hz and 10 kV/cm



($\sim 10^9 \Omega \text{ cm}$), in the case of thinner samples some heating was observed during measurement of the field induced strain characteristics, at a cycling frequency of 0.1 Hz, at 10 kV/cm. The dielectric loss and gross resistivity do not entirely explain the observed heating during measurement at the high field gradients $\sim 10\text{--}15$ kV/cm. It is plausible, however, that percolative channels may develop in the thin samples, which under the high field conditions could lead to joule heating. Under such conditions, thermal expansion effects could contribute also to axial displacements. For the samples tested, however, the displacement curves were symmetrical and without the distortion that might be expected from thermal effects being present.

4 Conclusions

1. The doping of BT ceramics with Nd_2O_3 and ZrO_4 at appropriate concentrations, has been demonstrated to produce materials of very high strain. Values of d_{33} exceeding 500 pCN^{-1} , exceptionally high for a lead free piezoceramic were realized.
2. The higher electromechanical responses in three layered systems compared to two layered ones, indicate that adjustment of compositional grading could result further improvements in amplification of strain response. Ceramics made by the procedure described, exhibit distinct compositionally variant layers with

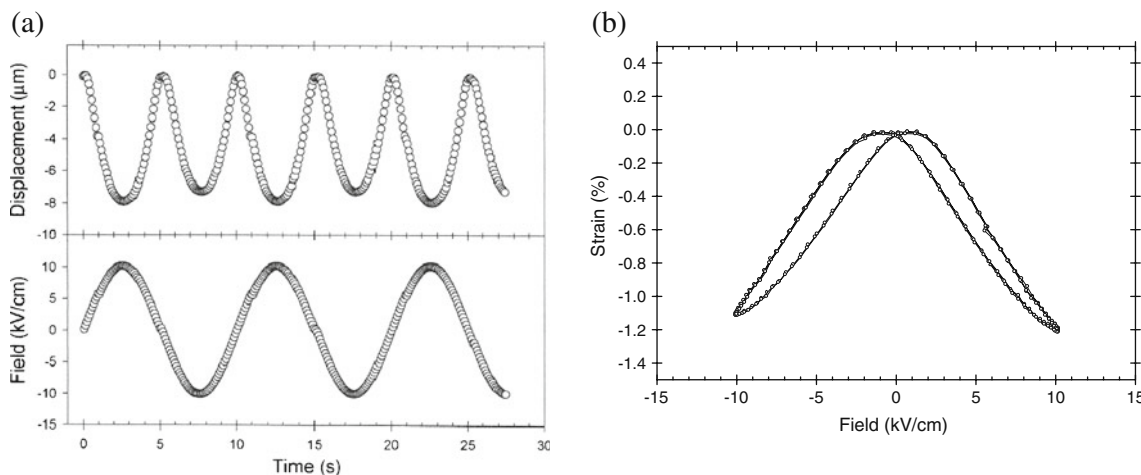


Fig. 6 Strain responses of Nd/Zr doped, 0.066 cm thickness three layered structure dome-down at 0.1 Hz and 10 kV/cm

- diffuse boundaries, due to diffusion during sintering. Furthermore, these functionally graded actuators were processed in one single sintering step.
3. Reduction of the overall disc thickness greatly enhances the displacement, but limitations are encountered in disc fabrication, handling, and likely heating effects that could contribute to d_{31} . Understanding these limitations could greatly expand development and use of these Nd-Zr doped BT for practical actuators.

Acknowledgement Funding for this work came from the National Science Foundation (NSF) under grants # DMR-0407569 and DMR-0805127. This financial support is gratefully acknowledged.

References

1. C. Niegrecki, D. Brei, S. Balakrishnan, A. Mosakalik, Shock. Vib. **33**, 269 (2001)
2. R.W. Schwartz, J. Ballato, G.H. Haertling, *Piezoelectric and electro-optic ceramics in ceramic materials for electronics*, ed. by R. Buchanan (Marcel Dekker, New York, 1998)
3. K. Uchino, Acta. Mater. **46**, 3745 (1998)
4. C.C.M. Wu, M. Kahn, W. Moy, J. Am. Ceram. Soc. **79**, 809 (1996)
5. K. Uchino, M. Yoshizaki, K. Kasai, H. Yamamura, N. Sakai, H. Asakura, Jpn. J. Appl. Phys. **26**, 1046 (1987)
6. G.H. Haertling, Am. Ceram. Soc. Bull. **73**, 93 (1994)
7. G. Li, E. Furman, G.M. Haertling, Ferroelectrics **182**, 69 (1996)
8. E. Catherine, L.E. Cross, C.A. Randall, J. Am. Ceram. Soc. **79**, 2041 (1996)
9. S.E. Park, T.R. Shrout, J. Appl. Phys. **82**, 1804 (1998)
10. R.F. Service, Science **275**, 1878 (1997)
11. P. Kumar, C. Prakash, T.C. Goel, Sci. Technol. Adv. Mat. **8**, 463 (2007)
12. X. Zhu, Q. Wang, Z. Meng, J. Mater. Sci. Lett. **14**, 516 (1995)
13. S.A. Wise, Sen. Actuators A **69**, 33 (1998)
14. J. Palosaari, J. Juuti, E. Heinonen, V.P. Moilanen, H. Jantunen, J. Electroceram. **22**, 156 (2009)
15. J. Qiu, J. Tani, T. Morita, H. Takahashi, H. Du, Smart. Mater. Struct. **12**, 115 (2003)
16. M. Taya, A.A. Almajd, M. Dunn, H. Takahashi, Sensors and Actuators A **107**, 248 (2003)
17. W. Preis, A. Burgermeister, W. Sitte, P. Supancic, Solid-State Ionics **173**, 69 (2004)
18. F.D. Morrison, D.C. Sinclair, A.R. West, J. Appl. Phys. **86**, 6355 (1999)
19. W. Heywang, J. Am. Ceram Soc. **47**, 484 (1964)
20. H. Hirose, J.M.S. Skakle, A.R. West, J. Electroceram **3**, 233 (1999)
21. Y. Lai, X. YaO, L. Zhang, Ceram. International **30**, 1325 (2004)
22. Z. Yao, H. Liu, Y. Liu, Z. Wu, Z. Shen, Y. Liu, M. CaO, Mater. Chem. Phys. **109**, 475
23. P. Murugaraj, T.R.N. Kutty, Diffuse phase transformation in neodymium-doped BaTiO₃ Ceramics. J. Mater. Sci. **21**, 3521 (1986)
24. T.R. Armstrong, L.E. Morgens, A.K. Maurice, R.C. Buchanan, J. Am. Ceram Soc. **72**, 605 (1989)
25. C. Gomez-Yanez, E.C. Aquino, J.J. Cruz-Rivera, R. Linares-Miranda, J. Alloys Compounds **434**, 806 (2007)
26. Y. Avrahami, H.L. Tuller, J. Electroceram **13**, 463 (2004)
27. V. Tura, L. Mitoseru, Europhysics. Lett. **50**, 810 (2000)
28. R.W. Schwartz, L.C. Cross, Q.M. Wang, J. Am. Ceram. Soc. **84**, 2563 (2001)
29. E. Steinhaus, S.G. Lipson, J. Opt. Soc. Am. **69**, 478 (1979)
30. E.N. Ribak, C. Schwartz, S.G. Lipson, The bimorph mirror-theoretical limits and technical aspects, Proc. 8th Meeting on Optical Engineering in Israel, SPIE vol.1971 pp 460–461